Hindawi
Shock and Vibration
Volume 2023, Article ID 7795452, 19 pages
https://doi.org/10.1155/2023/7795452

Research Article

Frequency-Based Cable Tension Identification Using a Nonlinear Model with Complex Boundary Constraints

Wen-ming Zhang and Zhi-wei Wang

The Key Laboratory of Concrete and Prestressed Concrete Structures of the Ministry of Education, Southeast University, Nanjing, China

Correspondence should be addressed to Wen-ming Zhang; zwm@seu.edu.cn

Received 17 August 2022; Revised 4 January 2023; Accepted 21 January 2023; Published 11 February 2023

Academic Editor: Luca Landi

Accurate estimation of the cable force affects the bridges' long-term integrity and serviceability directly. The frequency method is often used for cable tension testing in bridge engineering. However, the generally used cable tension calculation formulae are based on "ideal hinge" or "ideal fixed" boundary conditions. The inclination, bending stiffness, and sag-extensibility of the cable are not properly considered, which results in non-negligible errors. A frequency-based method for precisely determining the tensile force of a cable with unknown rotational and support constraint stiffnesses at the boundary was proposed. A nonlinear mathematical model of the vibration of the cable was established. In addition to parameters such as inclination, sag, and bending stiffness, the effects of unknown rotational and support constraint stiffnesses at both ends of the cable were also considered. The finite difference method was employed to discretize and solve the mode equation of the cable vibration. A frequency-based sensitivity-updating algorithm was applied that can identify simultaneously several system parameters using multiorder measured natural frequencies. Calculation of the matrix eigenvalue derivatives was the key to obtaining the system sensitivity matrix. Numerical examples indicated that the algorithm can be used efficiently and precisely to identify multiple system parameters of the cable, including its tension, bending stiffness, and boundary constraint stiffnesses.

1. Introduction

Cables are widely used in bridge engineering, for applications such as stay cables for cable-stayed bridges, flexible hangers for tied-arch bridges, and hangers for suspension bridges. The accuracy of the cable force testing affects the bridge construction monitoring, the structural stress state assessment, and the maintenance strategy formulation. Based on the basic principle that there is specific correspondence between the natural vibration frequencies and the cable tension, the cable tension can be determined by the measurement of the vibration frequencies. The frequency-based method is simple in operation and low in cost during bridge construction and service. In consequence, the approach is widely used for tension testing. However, practical applications have shown that the frequency-based method may produce non-negligible errors, mainly because of the inclination, sag-extensibility, bending stiffness, and boundary conditions of the cable have not been properly considered. Especially for applications with short and thick (high linear stiffness) cables, e.g., the short hangers of suspension bridges, this method has been observed to have low accuracy and may even lead to completely incorrect results. The main reason is that the vibration frequencies of the short hangers are particularly affected by boundary constraint stiffnesses.

In the earlier research, there were mainly three classical calculation theories of the frequency-based method. (1) The flat taut string theory neglects the influence of bending stiffness and sag-extensibility of the cable. The cable tension is obtained directly according to the measured frequency and frequency order. It applies only to flat and slender cables with low bending stiffness. (2) The axial-loaded slender beam theory considers the influence of bending stiffness but

ignores the sag-extensibility of the cable. It also requires the boundary condition to be ideally hinged or fixed. Several researchers studied the cable with pinned end conditions at the two ends [1, 2] and the cable with fixed end conditions at the two ends [3–5]. However, in engineering, the boundary conditions of the cable mostly show unknown rotational and support constraint stiffnesses. For example, one end of the anchorage cable strand of a suspension bridge is connected to the cantilever linkage of the front anchor facet. The opposite end is stacked with the other strands in the saddle groove and the "bearings" at both the ends of the cable vibrate in pace with the vibration of the cable. (3) The last approach is the application of practical calculation formulae that consider the bending stiffness and sag effect of the cable. However, to use these formulae, the bending stiffness and axial stiffness of the cable must be known. In practical engineering, the deformation mechanism of a beam and that of a cable are not exactly the same. Therefore, the use of the formulae for a beam to calculate the axial stiffness and bending stiffness of a cable is not always trustworthy.

Many researchers have conducted in-depth research on the vibration method for the estimation of cable tension. Irvine et al. [6] systematically studied the out-of-plane and in-plane linear vibration of the cable with a sag-to-span ratio of within $1:8$ and verified the theoretical correctness through experiments. Shimada and Nishimura [7] explored the influence of cable bending stiffness on cable tension estimation through experimental research. They found that a larger error resulted when using the vibration method to estimate the tensile force of a short cable, as the method ignores bending stiffness. Zui et al. [3] expressed the physical properties of the cable in the form of dimensionless parameters. They derived practical formulae for cable tensile force estimation which were presented by piece-wise functions and suitable for any cable regardless of the tensile force and the length of the cable. Mehrabi and Tabatabai [8] introduced a finite difference method for discretizing the vibration mode equation of the horizontal cable. A lot of important parameters such as the sag, bending stiffness, and the intermediate dampers or springs of the cable were taken into account. Based on the energy method and the curve fitting method, Ren et al. [4] gave empirical formulae adopting only the fundamental frequency of the cable.

Many difficulties in cable tension estimation will be imposed by the unknown complex boundary conditions when adopting the traditional cable force identification methods. Yan et al. [9] developed an innovative methodology independent of the cable boundary conditions. The problem of identifying the cable force was transformed into searching the zero-amplitude points from the mode shapes of the cable in their research. Chen et al. [10] put forward a new approach for cable tension identification using mode shape functions to eliminate the effects of complex boundary conditions. They considered that the cable with complex boundary conditions can be generally predicted by adopting an explicit formula of an equivalent cable model with pinned end conditions at the two ends. The abovementioned research attempted to give practical formulae for estimating the cable tension based on the vibration method but did not consider systematically the effects of cable inclination, bending stiffness, sag-extensibility, and the unknown boundary constraint stiffnesses on the dynamic characteristics of the vibration of the cable. Therefore, their applications have relatively large limitations.

In recent years, some numerical iterative algorithms which can estimate cable tensile force, bending stiffness, and some other parameters of the cable have been put forward. Kim and Park [11] established a finite element model taking into account the bending stiffness and sag effect of the cable. A frequency-based sensitivity-updating algorithm was adopted to determine the parameters of the cable model from the measured multiorder frequencies. Liao et al. [12] eliminated the errors between the frequencies calculated by an accurate finite element model of the cable and the measured frequencies by adopting a least squares optimization technique. This method can also determine the cable tension and other system parameters simultaneously. Li et al. [13] put forward an extended Kalman filter algorithm that can identify the cable tension varying with time in real-time. Zarbaf et al. [14] introduced an error function that corresponds to the differences between the calculated frequencies and the measured frequencies of the stay cable. Then, the particle swarm optimization algorithm and genetic algorithm were employed to minimize the error function and obtain the cable tension. However, the models established in these studies still did not consider systematically cable inclination, sag effect, bending stiffness, and the unknown boundary constraint stiffnesses at the cable end.

The technique developed in the present paper solves the disadvantages of classical theories. Compared with some modern cable theories, this paper established a nonlinear analytical model of the cable vibration which accurately accounted not only for the cable's inclination, bending stiffness, and sag effect but also for the influence of unknown rotational constraint stiffness and lateral support stiffness at the cable ends. The finite difference method was utilized to discretize the vibration mode equation of the cable, which transformed the complex analytical solution process into a simple numerical solution process. On this basis, the frequency-based sensitivity-updating algorithm could be used to identify simultaneously and accurately multiple system parameters of the cable according to multiple measured frequencies, including the cable tensile force, axial stiffness, bending stiffness, and unknown rotational and lateral stiffnesses at the cable end. Finally, the effectiveness and feasibility of the method developed in the present paper were verified by numerical examples.

2. Overall Idea

The overall idea of the method put forward in the present paper is shown in Figure 1. First, an analysis of the free vibration of the cable was conducted to establish the free vibration equation. The equation considers the inclination, bending stiffness, and sag-extensibility of the cable, which then was converted into a vibration mode equation by the mode separation method. Second, the boundary constraint equilibrium equations at the cable ends were established.

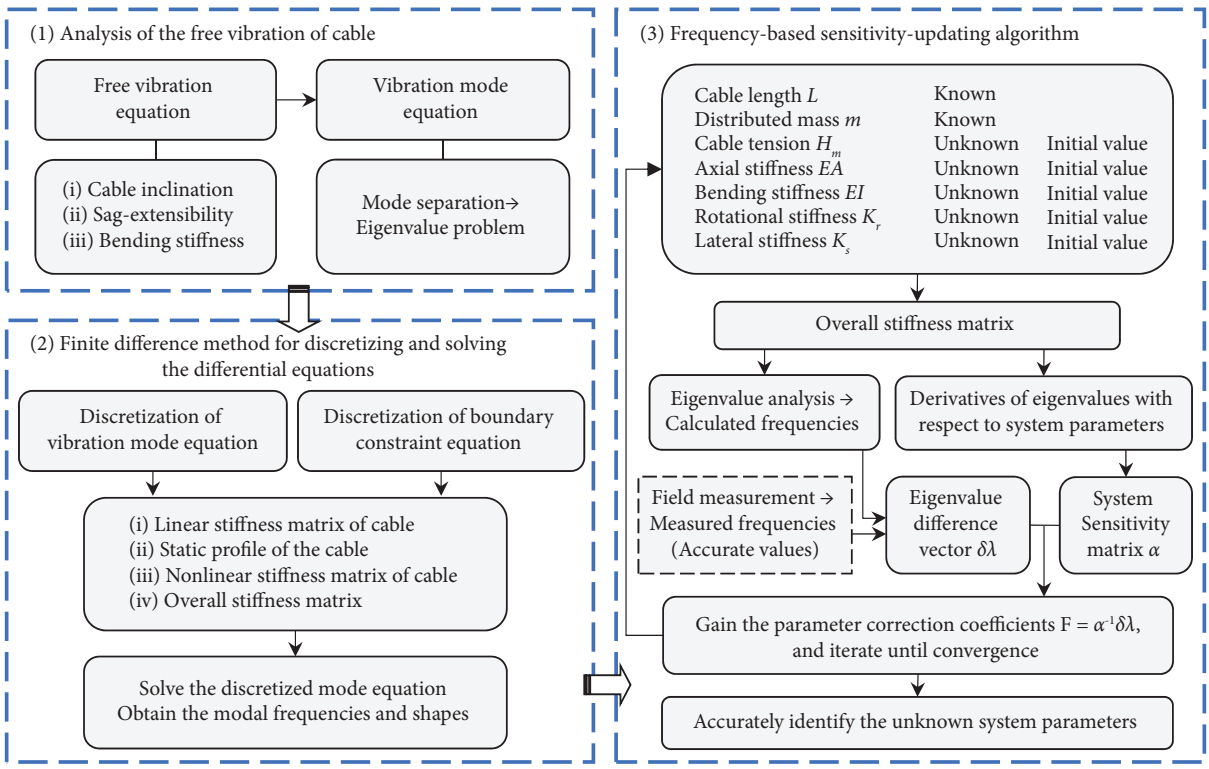

Figure 1: Overall idea flowchart.

Then, the finite difference method was used to discretize the vibration mode equation and the boundary constraint equilibrium equations to obtain the overall stiffness matrix of the cable. After the discretized vibration mode equation was established, the modal frequencies and mode shapes could be determined by eigenvalue analysis. Finally, a frequency-based sensitivity-updating algorithm was applied to identify simultaneously several system parameters using multiorder measured natural frequencies, including cable tension, axial stiffness, bending stiffness, and cable-end constraint stiffnesses.

The frequency-based sensitivity-updating algorithm for cable parameter identification is based on the concept of the Newton–Raphson method. Its derivative-based root-finding feature gives the algorithm a satisfactory convergence speed. Herein, the "sensitivity" refers to the variation of the cable's vibration eigenvalues (frequencies) along with the cable parameters; and the "updating" denotes the automatic update of the cable parameters with the help of the eigenvalue sensitivity matrix $\boldsymbol{\alpha}$ in each iteration. The detailed process is described as follows. First, proper initial iterative values of the system parameters were set to gain the initial overall stiffness matrix of the cable. Second, the eigenvalue analysis was conducted to obtain the eigenvalue difference vector $\delta\boldsymbol{\lambda}$ which represents the differences between the calculated and measured vibration eigenvalues. Third, the derivatives of the vibration eigenvalues with respect to the system parameters were calculated, and then, the eigenvalue sensitivity matrix $\boldsymbol{\alpha}$ was obtained. Essentially, $\boldsymbol{\alpha}$ is the Jacobian matrix representing the fastest decreasing direction of the eigenvalue difference $\delta\boldsymbol{\lambda}$ (or say the fastest convergent direction) in the solution space during the iteration. Finally, the correction coefficient of each cable parameter (denoted by $\mathbf{F}$) could be determined based on $\boldsymbol{\alpha}$ and $\delta\boldsymbol{\lambda}$. The initial iterative values of the cable parameters for the second iteration could be gained using $\mathbf{F}$ obtained from the first iteration. The above-mentioned process was repeated until convergence, and then, the accurate values of the system parameters were obtained. This algorithm could run automatically and efficiently when the appropriate initial iterative values were first determined.

3. Methodology

3.1. Free Vibration Analysis

3.1.1. Free Vibration Equation. Figure 2 shows the schematic of an inclined cable model along with the coordinate system. Point A is taken as the coordinate origin. Compared with the previous study [6–8], the proposed model gives systematic consideration to the inclination angle, bending stiffness, sag-extensibility, and geometric nonlinearity of the cable. Especially, the complex boundary constraints at the cable ends were first comprehensively modeled, which would be introduced in detail in Section 3.3.

Only the in-plane vibration of the cable is considered. Assume that it is uncoupled between the axial vibration and the transverse in-plane vibration of the cable. According to the D'Alembert principle, the equations of the chord-wise and transverse in-plane motions of the inclined cable are derived from the following equations:

$$\frac{\partial}{\partial s}\left[(T+\tau)\left(\frac{\mathrm{d}x}{\mathrm{d}s}+\frac{\partial u}{\partial s}\right)\right]+mg\sin\theta=m\frac{\partial^2 u}{\partial t^2}+c_u'\frac{\partial u}{\partial t}, \tag{1}$$

$$\frac{\partial}{\partial s}\left[(T+\tau)\left(\frac{\mathrm{d}y}{\mathrm{d}s}+\frac{\partial v}{\partial s}\right)\right]-\frac{\partial^2}{\partial s^2}\left(EI\frac{\partial^2\eta}{\partial x^2}\right)+mg\cos\theta=m\frac{\partial^2 v}{\partial t^2}+c_v'\frac{\partial v}{\partial t}, \tag{2}$$

where $T(x)$ denotes the initial cable tension; $\tau(x,t)$ denotes the additional tension caused by vibration; s is the arc-length coordinate; $y(x)$ denotes the static equilibrium profile; $u(x,t)$ and $v(x,t)$ represent the displacement in the x-direction and y-direction caused by vibration, respectively; $\eta(x,t)=y+v$ denotes the sum of the displacements in the y-direction; g denotes the gravitational acceleration; EI(x) denotes the bending stiffness; $m(x)$ denotes the mass per unit length; θ denotes the inclination angle; $c_u'(x)$ and $c_v'(x)$ represent the axial and transverse in-plane viscous damping coefficient per unit length, respectively. In addition, H_m denotes the mean value of the chord-wise component of $T(x)$; $EA(x)$ denotes the axial stiffness; and L denotes the cable length.

It is generally known that $T+\tau=(H+h)\mathrm{d}s/\mathrm{d}x$, where H and h denote the chord-wise component of T and τ, respectively. Furthermore, the axial vibration of the cable can be neglected. Then, equations (1) and (2) become

$$\frac{\partial}{\partial s}(H+h)+mg\sin\theta=0. \tag{3}$$

$$\frac{\partial}{\partial s}\left[(H+h)\left(\frac{\mathrm{d}y}{\mathrm{d}x}+\frac{\partial v}{\partial x}\right)\right]-\frac{\partial^2}{\partial s^2}\left(EI\frac{\partial^2\eta}{\partial x^2}\right)+mg\cos\theta=m\frac{\partial^2 v}{\partial t^2}+c_v'\frac{\partial v}{\partial t}. \tag{4}$$

If the sag-to-span ratio of the cable is no more than 1/10, ∂s can be replaced by ∂x. In this case, we can find that $\partial h/\partial x=0$ according to equation (3), therefore, $h(t)$ becomes a variable varying with time alone. Substituting the static equilibrium differential equation into equation (4) and neglecting the second-order terms results in

$$H(x)\frac{\partial^2 v}{\partial x^2}+H'(x)\frac{\partial v}{\partial x}+h\frac{\mathrm{d}^2 y}{\mathrm{d}x^2}-\frac{\partial^2}{\partial x^2}\left(EI\frac{\partial^2 v}{\partial x^2}\right)=m\frac{\partial^2 v}{\partial t^2}+c_v'\frac{\partial v}{\partial t}. \tag{5}$$

Equation (5) is the free vibration equation of an inclined cable, and the following steps are taken to transform it into an eigenvalue calculation.

3.1.2. Vibration Mode Equation. The vibration of a cable is the superposition of several modes, by using the mode separation method; the variable $v(x,t)$ can be expressed as follows:

$$v(x,t)=w(x)q(t), \tag{6}$$

where $w(x)$ denotes the mode shapes independent of time, and $q(t)$ denotes the generalized coordinates dependent on time alone. Considering the damped free vibration of a cable, q is generally written as $q(t)=\mathrm{e}^{pt}$, where $p=-\zeta\omega\pm\mathrm{i}\omega_D$, in which ζ denotes the damping ratio; ω and ω_D denote the nondamping and damped circular frequencies of the free vibration of the cable, respectively.

With the separation of the variable $v(x,t)$, equation (5) becomes

$$\frac{\mathrm{d}^2}{\mathrm{d}x^2}\left(EI\frac{\mathrm{d}^2 w}{\mathrm{d}x^2}\right)q-H\frac{\mathrm{d}^2 w}{\mathrm{d}x^2}q-H'\frac{\mathrm{d}w}{\mathrm{d}x}q-h\frac{\mathrm{d}^2 y}{\mathrm{d}x^2}+c_v'pwq+mp^2wq=0. \tag{7}$$

Expressing the additional cable tension component h as a linear correlation expression of the generalized coordinates q, then, the generalized coordinates q can be factored out as a common factor. Based on the relationship between the additional cable tension (τ) and the cable elongation, Irvine [1] derived the following expression:

$$\int_0^L\frac{h(\mathrm{d}s/\mathrm{d}x)^3}{EA}\mathrm{d}x=\int_0^L\frac{\partial u}{\partial x}\mathrm{d}x+\int_0^L\frac{\mathrm{d}y}{\mathrm{d}x}\frac{\partial v}{\partial x}\mathrm{d}x. \tag{8}$$

Due to the assumption that chord-wise displacement u equals zero, the first term of the right side of equation (8) is zero. As h is a variable varying with time alone, h can be written as follows:

$$h = \frac{\int_0^L (\mathrm{d}y/\mathrm{d}x)(\partial v/\partial x)\mathrm{d}x}{\int_0^L \left((\mathrm{d}s/\mathrm{d}x)^3/EA\right)\mathrm{d}x} = \frac{-\int_0^L \left(\mathrm{d}^2 y/\mathrm{d}x^2\right) w \mathrm{d}x}{\int_0^L \left(\left[(\mathrm{d}y/\mathrm{d}x)^2 + 1\right]^{3/2}/EA\right)\mathrm{d}x} q. \tag{9}$$

Substituting equation (9) into (7), eliminating the common factor q, and expanding the first term of equation (7) results in

$$\frac{\mathrm{d}^2(EI)}{\mathrm{d}x^2}\frac{\mathrm{d}^2 w}{\mathrm{d}x^2} + 2\frac{\mathrm{d}(EI)}{\mathrm{d}x}\frac{\mathrm{d}^3 w}{\mathrm{d}x^3} + EI\frac{\mathrm{d}^4 w}{\mathrm{d}x^4} - H\frac{\mathrm{d}^2 w}{\mathrm{d}x^2} - H'\frac{\mathrm{d}w}{\mathrm{d}x} + \frac{\int_0^L \left(\mathrm{d}^2 y/\mathrm{d}x^2\right) w \mathrm{d}x}{\int_0^L \left(\left[(\mathrm{d}y/\mathrm{d}x)^2 + 1\right]^{3/2}/EA\right)\mathrm{d}x}\frac{\mathrm{d}^2 y}{\mathrm{d}x^2} + c_v' p w + m p^2 w = 0. \tag{10}$$

Equation (10) is the nonlinear vibration mode equation of an inclined cable. The first five terms of the left side are the linear stiffness part of the cable while the sixth term denotes the nonlinear stiffness part. By using the finite difference method to discretize this fourth-order nonlinear differential equation, the eigenvalue problem will be solved by a numerical technique below.

3.2. Finite Difference Method for Discretizing the Mode Equation. The differential schemes of individual terms in equation (10) are transformed into difference schemes after using the finite difference method for discretization. Figure 3 shows a schematic of a discretized inclined cable with n internal nodes and $n+1$ segments. The projection length on the chord line of each cable segment is expressed as $a = L/(n+1)$.

Defining the difference schemes of mode shape functions $w(x)$ in the following forms:

$$\frac{\mathrm{d}w(x_i)}{\mathrm{d}x} = \frac{w_{i+1} - w_{i-1}}{2a}, \frac{\mathrm{d}^2 w(x_i)}{\mathrm{d}x^2} = \frac{w_{i+1} - 2w_i + w_{i-1}}{a^2}$$
$$\frac{\mathrm{d}^3 w(x_i)}{\mathrm{d}x^3} = \frac{w_{i+2} - 2w_{i+1} + 2w_{i-1} - w_{i-2}}{2a^3}, \frac{\mathrm{d}^4 w(x_i)}{\mathrm{d}x^4} = \frac{w_{i+2} - 4w_{i+1} + 6w_i - 4w_{i-1} + w_{i-2}}{a^4}. \tag{11}$$

Furthermore, the difference schemes of EI(x), EA(x), and $y(x)$ are the same as $w(x)$.

Converting the differential scheme into the difference scheme at node i ($i = 1, 2, \ldots, n$) by adopting the above-mentioned formulae, which then gives the matrix form of the discretized mode equation:

$$\mathbf{K}\mathbf{w} + \mathbf{C}p\mathbf{w} + \mathbf{M}p^2\mathbf{w} = 0. \tag{12}$$

In which,

$$\mathbf{K} = \mathbf{K}_1 + \mathbf{K}_2,$$
$$\mathbf{w}^{\mathrm{T}} = \{w_1, w_2, \ldots, w_n\};\ \mathbf{M} = \mathrm{diag}\{m_1, m_2, \ldots, m_n\};\ \mathbf{C} = \mathrm{diag}\{c_{v1}', c_{v2}', \ldots, c_{vn}'\}, \tag{13}$$

where $\mathbf{K_1}$ and $\mathbf{K_2}$ are the linear stiffness matrix and the nonlinear stiffness matrix, respectively; n represents the number of internal nodes; w_i and m_i denote the mode shape displacement and mass per unit length at node i ($i = 1, 2, \ldots, n$), respectively; $c_{vi}' = c_{vi}/a$, and c_{vi} denotes the transverse in-plane viscous damping coefficient of the damper at node i.

The linear stiffness matrix $\mathbf{K_1}$ is expressed as follows:

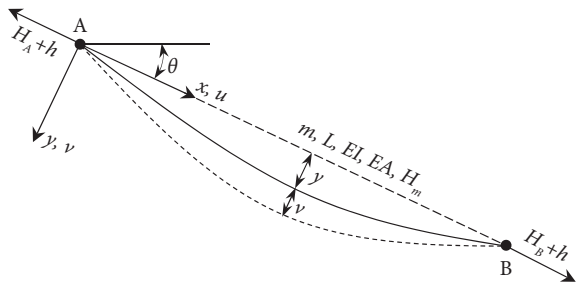

Figure 2: Schematic of an inclined cable.

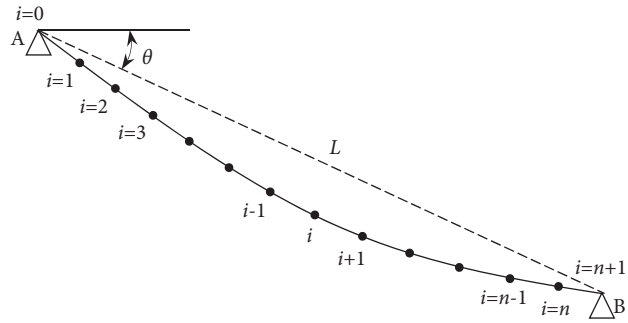

Figure 3: Schematic of a discretized inclined cable.

$$\mathbf{K}_1 = \begin{pmatrix} Q & U_1 & W_1 & & & & & & 0 \\ R & S_2 & U_2 & W_2 & & & & & \\ V_3 & D_3 & S_3 & U_3 & W_3 & & & & \\ & - & - & - & - & - & & & \\ & & V_i & D_i & S_i & U_i & W_i & & \\ & & & - & - & - & - & - & \\ & & & & V_{n-2} & D_{n-2} & S_{n-2} & U_{n-2} & W_{n-2} \\ & & & & & V_{n-1} & D_{n-1} & S_{n-1} & P \\ 0 & & & & & & V_n & D_n & T \end{pmatrix}_{n\times n}. \tag{14}$$

Each internal node of the discretization model of the cable corresponds to one row of $\mathbf{K_1}$, in which:

$$\begin{aligned} V_i &= -\frac{1}{2a^4}\left(EI_{i+1} - 2EI_i - EI_{i-1}\right) \\ W_i &= \frac{1}{2a^4}\left(EI_{i+1} + 2EI_i - EI_{i-1}\right) \\ S_i &= \frac{1}{a^4}\left(-2EI_{i+1} + 10EI_i - 2EI_{i-1}\right) + \frac{2H_i}{a^2} \\ D_i &= \frac{1}{a^4}\left(2EI_{i+1} - 6EI_i\right) - \frac{H_i}{a^2} + \frac{H_{i+1} - H_{i-1}}{4a^2} \\ U_i &= \frac{1}{a^4}\left(-6EI_i + 2EI_{i-1}\right) - \frac{H_i}{a^2} - \frac{H_{i+1} - H_{i-1}}{4a^2}, \end{aligned} \tag{15}$$

where EI_i and H_i are the bending stiffness and the chord-wise component of the cable tensile force at the internal node i, respectively. D and U incorporate the effect associated with the inclined angle of the cable, compared with previous research on horizontal cables [8]. Meanwhile, the effect of the boundary conditions is incorporated into Q, T, R, and P. The expressions for them need to be determined based on the boundary equilibrium equations described below.

The nonlinear stiffness matrix $\mathbf{K_2}$ is expressed as follows:

$$\mathbf{K}_2 = \mathbf{r}\mathbf{s}^{\mathrm{T}};\ \mathbf{r}^{\mathrm{T}} = \{r_1, r_2, \ldots, r_n\};\ \mathbf{s}^{\mathrm{T}} = \{s_1, s_2, \ldots, s_n\}, \tag{16}$$

in which,

$$r_i = \frac{s_i}{\sum_{i=1}^{n} t_i^3/EA_i};\ s_i = \frac{y_{i+1} - 2y_i + y_{i-1}}{a^2};\ t_i = \left\{\left[\left(y_{i+1} - y_{i-1}\right)/2a\right]^2 + 1\right\}^{1/2}. \tag{17}$$

It is necessary to solve the static equilibrium profile due to the self-weight of the cable because some of the terms used depend on y as is reflected in the expressions for $\mathbf{K_2}$.

When the damping ratio ζ is very small, the effect of damping can be neglected. At this time, the damped circular frequencies ω_D is equal to the undamped circular frequencies ω of the free vibration of the cable, and $p^2 = -\omega^2$. Then, equation (12) becomes

$$\mathbf{K}\mathbf{w} - \mathbf{M}\omega^2\mathbf{w} = 0, \tag{18}$$

Equation (18) indicates that the modal frequencies and the mode shapes of a cable in free vibration are the generalized eigenvalues and eigenvectors of the mass matrix and stiffness matrix of a cable, respectively.

3.3. Boundary Constraint Equilibrium Equations. In order to calculate the elements Q, T, R, and P in the matrix $\mathbf{K_1}$, the boundary conditions of the cable should be taken into account.

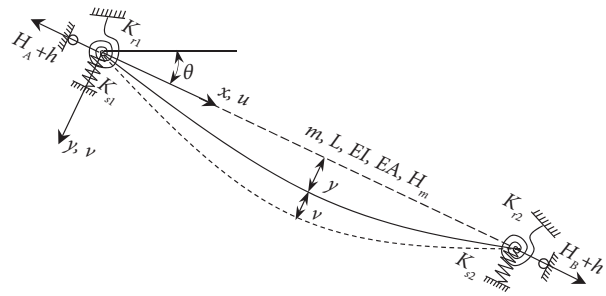

Figure 4: Schematic of a cable under the boundary of elastic embedding and elastic support.

In practical engineering, the constraints at the cable ends are usually neither simply pinned nor completely fixed. Herein, it is assumed that the boundary conditions of the cable are elastic support and elastic embedding at both ends. Figure 4 shows an inclined cable model under the boundary conditions of elastic support and elastic embedding, in which K_{r1} and K_{r2} are the rotational stiffness at the cable ends, and K_{s1} and K_{s2} are the lateral support stiffness at the cable ends.

According to the equilibrium of the moment and shear force at the two ends of the cable, the boundary constraint equilibrium equations of the cable are derived as follows:

$$K_{r1}\left.\frac{\mathrm{d}w}{\mathrm{d}x}\right|_{x=0} - EI\left.\frac{\mathrm{d}^2w}{\mathrm{d}x^2}\right|_{x=0} = 0, K_{s1}w|_{x=0} - H\left.\frac{\mathrm{d}w}{\mathrm{d}x}\right|_{x=0} + EI\left.\frac{\mathrm{d}^3w}{\mathrm{d}x^3}\right|_{x=0} = 0, \tag{19}$$

$$K_{r2}\left.\frac{\mathrm{d}w}{\mathrm{d}x}\right|_{x=l} + EI\left.\frac{\mathrm{d}^2w}{\mathrm{d}x^2}\right|_{x=l} = 0, K_{s2}w|_{x=l} + H\left.\frac{\mathrm{d}w}{\mathrm{d}x}\right|_{x=l} - EI\left.\frac{\mathrm{d}^3w}{\mathrm{d}x^3}\right|_{x=l} = 0. \tag{20}$$

After discretizing the calculation model of the cable, equations (19) and (20) become

$$K_{r1}\frac{w_1 - w_{-1}}{2a} - EI_0\frac{w_1 - 2w_0 + w_{-1}}{a^2} = 0, \tag{21}$$

$$K_{s1}w_0 - H_0\frac{w_1 - w_{-1}}{2a} + K_{r1}\frac{w_1 - 2w_0 + w_{-1}}{a^2} = 0, \tag{22}$$

$$K_{r2}\frac{w_{n+2} - w_n}{2a} + EI_{n+1}\frac{w_{n+2} - 2w_{n+1} + w_n}{a^2} = 0, \tag{23}$$

$$K_{s2}w_{n+1} + H_{n+1}\frac{w_{n+2} - w_n}{2a} + K_{r2}\frac{w_{n+2} - 2w_{n+1} + w_n}{a^2} = 0. \tag{24}$$

To determine the elements Q and T, one should replace w_{-1} and w_0 with a factor containing w_1 and replace w_{n+1} and w_{n+2} with a factor containing w_n. Analogously, to determine the elements R and P, w_0 should be expressed by a factor containing w_1, and w_{n+1} should be expressed by a factor containing w_n. Based on equations (23)–(26), one can obtain the following equations:

$$\begin{cases} w_0 = \dfrac{2EI_0H_0 - 2K_{r1}^2}{K_{s1}a\left(K_{r1}a + 2EI_0\right) + 2EI_0H_0 - 2K_{r1}^2}w_1 \\ w_{-1} = \dfrac{K_{r1}a - 2EI_0}{K_{r1}a + 2EI_0}w_1 + \dfrac{4EI_0}{K_{r1}a + 2EI_0}\cdot\dfrac{2EI_0H_0 - 2K_{r1}^2}{K_{s1}a\left(K_{r1}a + 2EI_0\right) + 2EI_0H_0 - 2K_{r1}^2}w_1 \end{cases}$$

$$\begin{cases} w_{n+1} = \dfrac{2EI_{n+1}H_{n+1} - 2K_{r2}^2}{K_{s2}a\left(K_{r2}a + 2EI_{n+1}\right) + 2EI_{n+1}H_{n+1} - 2K_{r2}^2}w_n \\ w_{n+2} = \dfrac{\left(K_{r2}a - 2EI_{n+1}\right)}{K_{r2}a + 2EI_{n+1}}w_n + \dfrac{4EI_{n+1}}{K_{r2}a + 2EI_{n+1}}\cdot\dfrac{2EI_{n+1}H_{n+1} - 2K_{r2}^2}{K_{s2}a\left(K_{r2}a + 2EI_{n+1}\right) + 2EI_{n+1}H_{n+1} - 2K_{r2}^2}w_n. \end{cases} \tag{25}$$

Then, the elements Q, T, R, and P in the matrix $\mathbf{K_1}$ can be determined as follows:

$$Q = S_1 + \frac{K_{r1}a - 2EI_0}{K_{r1}a + 2EI_0}V_1 + \frac{2EI_0H_0 - 2K_{r1}^2}{K_{s1}a\left(K_{r1}a + 2EI_0\right) + 2EI_0H_0 - 2K_{r1}^2}\left(D_1 + \frac{4EI_0}{K_{r1}a + 2EI_0}V_1\right), \tag{26}$$

$$T = S_n + \frac{K_{r2}a - 2EI_{n+1}}{K_{r2}a + 2EI_{n+1}}W_n + \frac{2EI_{\mathrm{n}+1}H_{\mathrm{n}+1} - 2K_{r2}^2}{K_{s2}a\left(K_{r2}a + 2EI_{\mathrm{n}+1}\right) + 2EI_{\mathrm{n}+1}H_{\mathrm{n}+1} - 2K_{r2}^2}\left(U_n + \frac{4EI_{\mathrm{n}+1}}{K_{r2}a + 2EI_{n+1}}W_n\right), \tag{27}$$

$$R = D_2 + \frac{2EI_0H_0 - 2K_{r1}^2}{K_{s1}a\left(K_{r1}a + 2EI_0\right) + 2EI_0H_0 - 2K_{r1}^2}V_2, \tag{28}$$

$$P = U_{n-1} + \frac{2EI_{n+1}H_{n+1} - 2K_{r2}^2}{K_{s2}a\left(K_{r2}a + 2EI_{n+1}\right) + 2EI_{n+1}H_{n+1} - 2K_{r2}^2}W_{n-1}, \tag{29}$$

where EI_0 and EI_{n+1} denote the bending stiffness at the two ends, and H_0 and H_{n+1} denote the chord-wise component of the cable tensile force at the two ends.

3.4. Static Profile of the Cable. One of the premises of finding the value of each element in the stiffness matrix $\mathbf{K_2}$ is to obtain the static displacement y_i ($i = 1, 2, \ldots, n$) of each node of the cable under the static equilibrium state. That is, it is necessary to calculate the static equilibrium profile due to the self-weight of the cable. The static profile is often presumed to be a parabola [1]. This assumption is appropriate when the cable is an equal-section horizontal cable that does not consider the bending stiffness. However, when the bending stiffness of the cable cannot be neglected, or the sectional characteristic varies along the cable, the true static profile of the cable will deviate significantly from the parabola. Therefore, the finite difference method is employed to calculate the static profile of the cable in this study.

The static equilibrium differential equation of an inclined cable subjected to tension is as follows:

$$\frac{\mathrm{d}^2}{\mathrm{d}x^2}\left(EI\frac{\mathrm{d}^2y}{\mathrm{d}x^2}\right) - H\frac{\mathrm{d}^2y}{\mathrm{d}x^2} = mg\cos\theta. \tag{30}$$

Similar to the discretization of the vibration mode equation, the abovementioned equation can also be written in the following matrix form:

$$\mathbf{K}_s\mathbf{y} = \mathbf{m}g\cos\theta \text{ in which, } \mathbf{y}^{\mathrm{T}} = \{y_1, y_2, \ldots, y_n\};\ \mathbf{m}^{\mathrm{T}} = \{m_1, m_2, \ldots, m_n\}, \tag{31}$$

where $\mathbf{K_s}$ is the static stiffness matrix. This is basically the same as for $\mathbf{K_1}$ in equation (14) but with the expressions for elements D_i and U_i in the matrix modified as follows:

$$D_i = \frac{1}{a^4}\left(2EI_{i+1} - 6EI_i\right) - \frac{H_i}{a^2};\ U_i = \frac{1}{a^4}\left(-6EI_i + 2EI_{i-1}\right) - \frac{H_i}{a^2}. \tag{32}$$

According to equation (31), the static profile can be calculated for solving the vibration mode equation.

3.5. Multiparameter Identification Algorithm. To accurately identify the cable tension utilizing the measured frequencies in situ, it is necessary to identify some other parameters in the cable vibration system besides the cable tension. The deformation mechanism of a beam and that of a cable are not exactly the same, thus, it is not always trustworthy to use the formulae for a beam to compute the axial stiffness and bending stiffness of a cable. Hence, the mean value of the chord-wise component of the cable tension H_m, the axial stiffness EA, the bending stiffness EI, the rotational constraint stiffness, K_{r1} and K_{r2}, at the two ends of the cable, and the lateral support stiffness, K_{s1} and K_{s2}, at the two ends of the cable, were selected to be the physical parameters that need to be identified in the cable vibration system. A frequency-based sensitivity-updating algorithm was applied for the multiparameter identification of the cable using multi-order frequencies, as shown in Figure 5.

The physical parameters to be identified in the cable vibration system constitute the parameter vector $\mathbf{X}$ of the order of $p \times 1$:

$$\mathbf{X} = \left\{ H_m \;\; EI \;\; EA \;\; K_{r1} \;\; K_{r2} \;\; K_{s1} \;\; K_{s2} \right\}^{\mathrm{T}}. \tag{33}$$

Assuming that for the n^{th}-order vibration eigenvalue $\lambda_n = \omega_n^2$, then, the variation of λ_n is as follows:

$$\delta\lambda_n = \lambda_n(\mathbf{X} + \Delta\mathbf{X}) - \lambda_n(\mathbf{X}). \tag{34}$$

Performing Taylor expansion on the first term of the right side of equation (34), one can obtain the following:

$$\delta\lambda_n = \sum_{k=1}^{p} \frac{\partial \lambda_n}{\partial x_k} \Delta x_k = \sum_{k=1}^{p} \frac{\partial \lambda_n}{\partial x_k} x_k \frac{\Delta x_k}{x_k}, \tag{35}$$

where x_k is the k^{th} element of the parameter vector $\mathbf{X}$.

If N frequencies are used for the identification of system parameters, from equation (35) the following can be obtained:

$$\boldsymbol{\alpha}\mathbf{F} = \delta\boldsymbol{\lambda}, \tag{36}$$

in which,

$$\mathbf{F} = \left\{ \Delta x_1/x_1^{eva} \;\; \Delta x_2/x_2^{eva} \;\; \dots \;\; \Delta x_p/x_p^{eva} \right\}^{\mathrm{T}},$$

$$\delta\boldsymbol{\lambda} = \left\{ \delta\lambda_1 \;\; \delta\lambda_2 \;\; \dots \;\; \delta\lambda_N \right\}^{\mathrm{T}},$$

$$\boldsymbol{\alpha} = \begin{pmatrix} \frac{\partial \lambda_1}{\partial x_1} x_1^{eva} & \frac{\partial \lambda_1}{\partial x_2} x_2^{eva} & \cdots & \frac{\partial \lambda_1}{\partial x_p} x_p^{eva} \\ \frac{\partial \lambda_2}{\partial x_1} x_1^{eva} & \frac{\partial \lambda_2}{\partial x_2} x_2^{eva} & \cdots & \frac{\partial \lambda_2}{\partial x_p} x_p^{eva} \\ \vdots & \vdots & \vdots & \vdots \\ \frac{\partial \lambda_N}{\partial x_1} x_1^{eva} & \frac{\partial \lambda_N}{\partial x_2} x_2^{eva} & \cdots & \frac{\partial \lambda_N}{\partial x_p} x_p^{eva} \end{pmatrix}, \tag{37}$$

where x_k^{eva} is the initial evaluated value for the k^{th} element of $\mathbf{X}$.

The coefficient matrix $\boldsymbol{\alpha}$ in equation (36) is a Jacobian matrix combined with the initial evaluated values of cable parameters. The parameter vector $\mathbf{X}$ becomes a dimensionless vector $\mathbf{F}$ when the initial evaluated values of cable parameters are introduced into $\boldsymbol{\alpha}$. In this case, the sensitivity of vibration eigenvalues to the cable parameters is truly reflected in the coefficient matrix $\boldsymbol{\alpha}$, regardless of the absolute value of each element of $\mathbf{X}$. Introducing the initial values into $\boldsymbol{\alpha}$ is also an effective technique to decrease the condition number of $\boldsymbol{\alpha}$ and improve the stability of solving the linear equations numerically.

An iterative solution of equation (36) yields an accurate value for each parameter in the parameter vector $\mathbf{X}$, which comprises the following nine steps:

Step 1. Select the appropriate initial value of each parameter. Calculate H_m^{eva} according to the practical formula [3]. Calculate EI^{eva} and EA^{eva} according to the formulae in material mechanics for calculating the bending stiffness and the axial stiffness. The dimension of K_r is the same as the dimension of EI/a, and the dimension of K_s is the same as the dimension of EI/a^3. When the ratio of the K_r to EI/a exceeds 4.0, the frequencies of the cable are close to converging. Therefore, the search range of K_{r1}^{eva} and K_{r2}^{eva} can be set to be $[0.0, 4.0]\text{EI}/a$. Similarly, according to the result of the parameter sensitivity analysis, when the ratio of the K_s to EI/a^3 exceeds 20.0, the frequencies of the cable are close to converging. Therefore, the search range of K_{s1}^{eva} and K_{s2}^{eva} can be set to be $[0.0, 20.0]\text{EI}/a^3$. In practical engineering, it is essential to conduct a trial of convergence based on experience.

Step 2. Calculate the linear stiffness matrix $\mathbf{K_1}$ of the cable.

Step 3. Calculate the static profile of the cable.

Step 4. Calculate the nonlinear stiffness matrix $\mathbf{K_2}$ and obtain the overall stiffness matrix $\mathbf{K}$.

Step 5. Perform eigenvalue analysis and obtain the calculated eigenvalues λ_{tn} of the cable.

Step 6. Calculate $\delta\boldsymbol{\lambda}$ according to the following formula:

$$\delta\boldsymbol{\lambda} = \left\{ \lambda_{m1} - \lambda_{t1} \;\; \lambda_{m2} - \lambda_{t2} \;\; \dots \;\; \lambda_{mn} - \lambda_{tn} \;\; \dots \;\; \lambda_{mN} - \lambda_{tN} \right\}^{\mathrm{T}}, \tag{38}$$

where λ_{mn} is the measured value (i.e., accurate value) of the n^{th}-order eigenvalue and λ_{tn} is the n^{th}-order calculated eigenvalue after t iterations.

Step 7. Calculate the matrix $\boldsymbol{\alpha}$. Calculation of the vibration eigenvalue derivatives $\partial\lambda_n/\partial x_k$ is the key aspect of the calculation of matrix $\boldsymbol{\alpha}$. The analytical method for calculating the eigenvalue derivatives of the cable vibration will be described in detail in the Appendix.

Step 8. Calculate $\mathbf{F}$ according to equation (39). To obtain a definite solution for equation (39), the number of measured frequencies should be equal to or greater than the number of parameters to be estimated. When the number of measured frequencies is equal to the number of parameters to be identified, i.e., $N = p$, $\mathbf{F}$ can be solved by the following:

$$\mathbf{F} = \boldsymbol{\alpha}^{-1}\delta\boldsymbol{\lambda}. \tag{39}$$

When the number of measured frequencies is greater than the number of parameters to be identified, i.e., $N > p$, equation (36) becomes an overdetermined equation and can be solved by the least squares technique. The same method applies when $N = p$. The objective function of the least squares technique is the sum of squares of $\delta\lambda_n = (\lambda_{mn} - \lambda_{tn})$:

$$E = \sum_{n=1}^{N} (\delta\lambda_n)^2 = \delta\boldsymbol{\lambda}^{\mathrm{T}}\delta\boldsymbol{\lambda}. \tag{40}$$

According to the principle of the least squares technique, $\partial E/\partial\mathbf{F} = 0$, the following expression can be obtained:

$$\begin{aligned} &\mathbf{F} = \left(\boldsymbol{\alpha}^{\mathrm{T}}\boldsymbol{\alpha}\right)^{-1}\boldsymbol{\alpha}^{\mathrm{T}}\delta\boldsymbol{\lambda} \\ &F_{k,\min} < F_k < F_{k,\max} \; (k = 1, 2, \dots, p), \end{aligned} \tag{41}$$

where $F_{k,\ \min}$ and $F_{k,\ \max}$ are employed to constrain the search range of x_k. It is an efficient way to constrain the search ranges of parameters to enhance the robustness of the least squares technique. Based on the actual situation and engineering experience, the search range of x_k can be

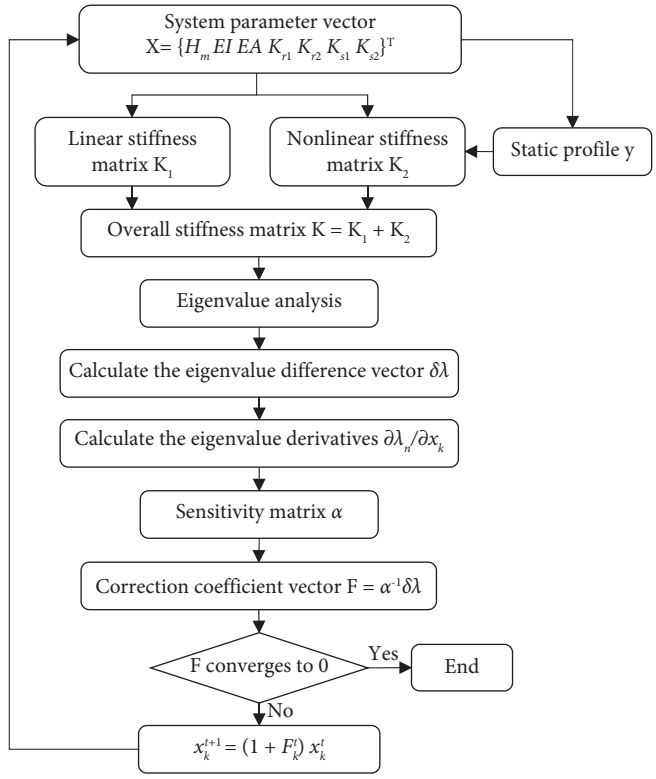

Figure 5: Block diagram of the sensitivity-updating algorithm for system parameter identification.

Table 1: Physical parameters of four numerical cables.

No	H_m (10^6N)	E (Pa)	A (m^2)	I (m^4)	λ^2	ξ
Cable 1	2.9036	$1.5988E+10$	$7.8507E-03$	$4.9535E-06$	0.79	605.5
Cable 2	0.7259	$1.7186E+10$	$7.611E-03$	$4.6097E-06$	50.70	302.7
Cable 3	26.13254	$2.0826E+13$	$7.8633E-03$	$4.9204E-06$	1.41	50.5
Cable 4	0.7259	$4.7834E+8$	$0.7345E-01$	$5.9506E-03$	50.70	50.5

Note. The nondimensional parameters λ^2 [3] and ξ [1] characterize the flexural stiffness and sag-extensibility of the cable, respectively. The cable sag-extensibility increases with λ^2, and the flexural stiffness decreases with ξ.

predetermined approximately. For instance, in the cable tension calculation, the error of H_m^{eva} with the calculation result using the practical formula [3] is generally within 20%. Therefore, the variation range of F_{H_m} can be constrained to within [−0.2, +0.2].

Step 9. The following equation is used to obtain the values of corrected system parameters, which will be used in the $(t+1)^{\text{th}}$ iteration:

$$x_k^{t+1} = \left(1 + F_k^t\right) x_k^t, \tag{42}$$

where x_k^t is the k^{th} identification parameter of $\mathbf{X}^t$ after the t^{th} iteration. F_k^t is the k^{th} element of $\mathbf{F}^t$ after the t^{th} iteration.

The abovementioned steps are repeated until $\mathbf{F}$ approaches zero.

4. Case Study

4.1. Introduction to Numerical Cables. Four numerical cables with significantly different characteristics used in the previous studies [8, 11, 15] were adopted to evaluate the method of the present paper. Their main physical parameters are listed in Table 1. Except for those, they have the same length ($L = 100$ m) and mass per unit length ($m = 400$ kg/m). Moreover, the cables' inclination angles θ were all set to 30° and the damping of the cables was ignored. In the discretized model, the cable was divided into 100 segments along the x-direction, with a total of 99 internal nodes ($n = 99$ and $a = 1$ m).

It can be found in Table 1 that Cable 1 has small sag-extensibility and small flexural stiffness; Cable 2 has large sag-extensibility and small flexural stiffness; Cable 3 has small sag-extensibility and large flexural stiffness; and Cable 4 has large sag-extensibility and large flexural stiffness. They were believed to be able to cover a variety of cable features in practical engineering.

4.2. Influence of Boundary on Structural Behaviors

4.2.1. Influence on Cable's Static Profile. The static displacement y_i of the cable participated in the formation of matrix $\mathbf{K_2}$. In other words, the change of the cable's static

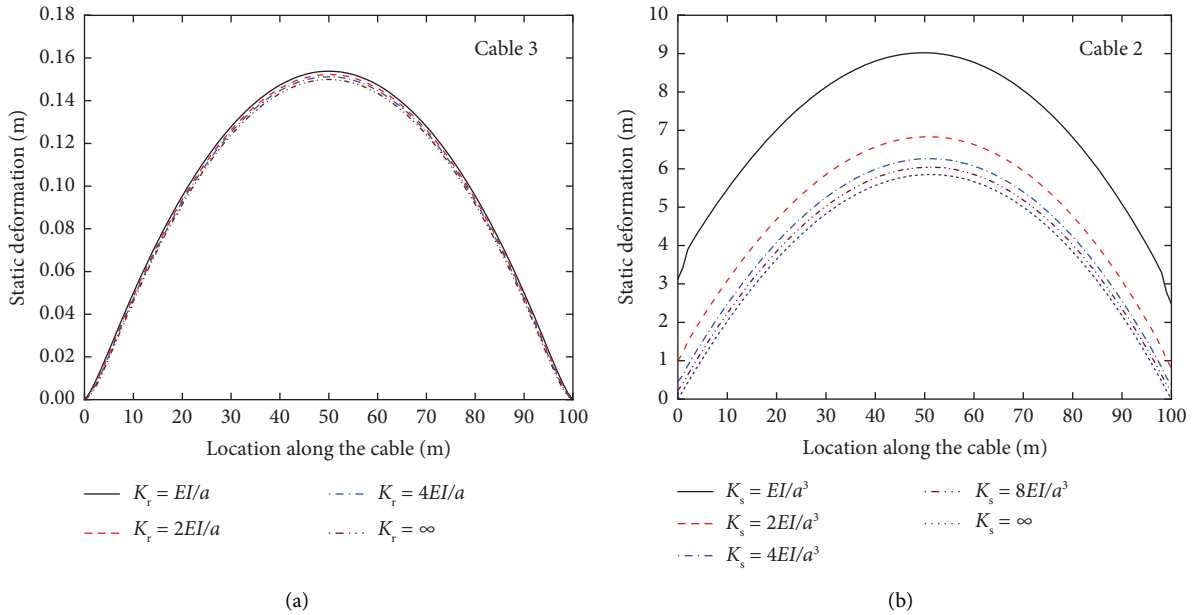

FIGURE 6: Influence of (a) rotational constraint stiffness K_r and (b) lateral support constraint stiffness K_s at the cable ends on cable's static profile.

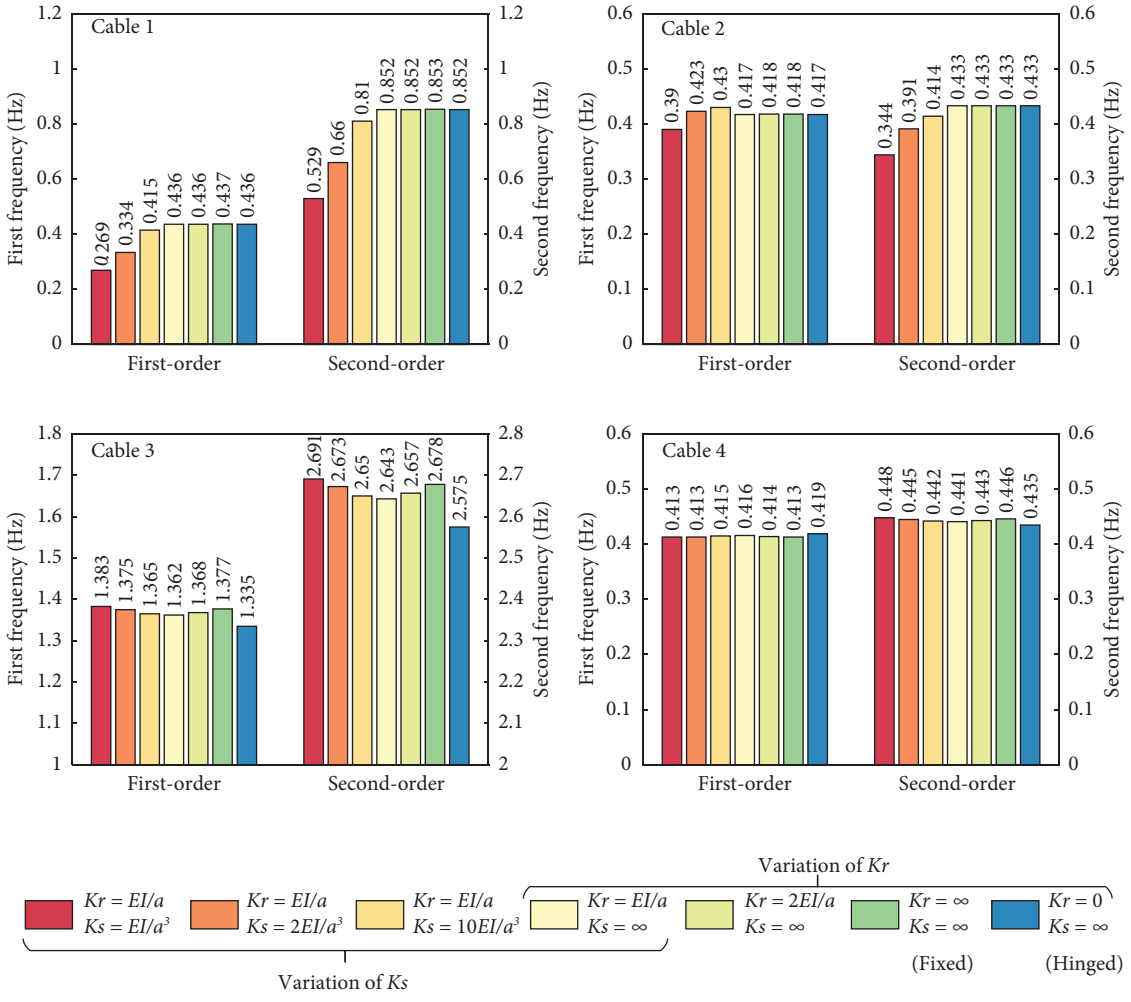

FIGURE 7: Influence of boundary constraint stiffnesses on cable's first two vibration frequencies.

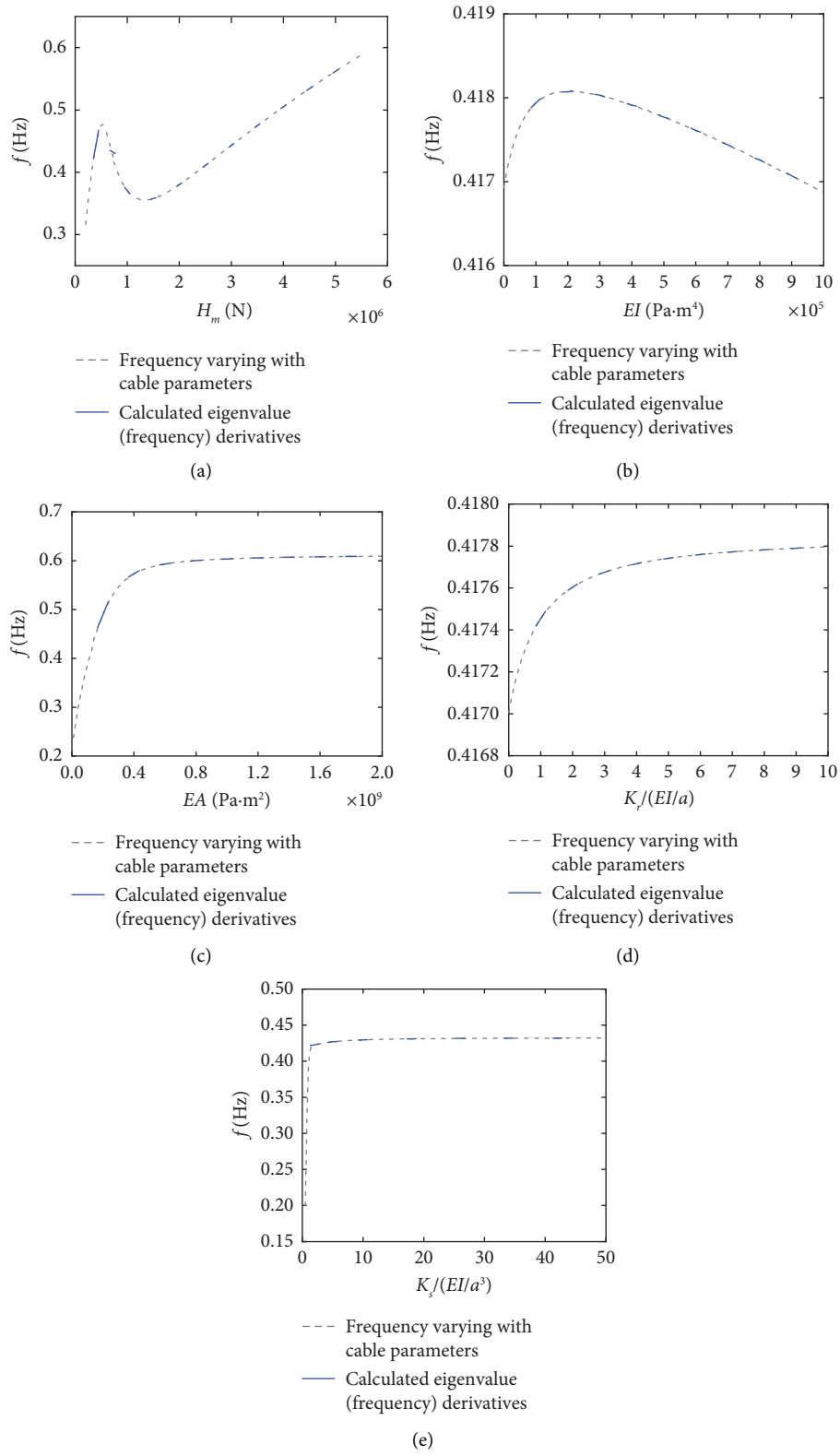

Figure 8: Illustration of calculated derivatives of the first eigenvalue (frequency) of cable 2 with respect to its system parameters: (a) H_m; (b) EI; (c) EA; (d) K_r; and (e) K_s.

profile caused by the variation of boundary conditions will affect the cable's nonlinear stiffness matrix. First, to investigate the effect of the rotational stiffnesses at the cable ends on the cable's static profile, taking Cable 3 as an example, assuming the boundary rotational stiffnesses K_r at two ends were the same and the boundary lateral

Table 2: Accurate and initial values of system parameters of the four cables.

No	Items	H_m (N)	EI (Pa•m^4)	EA (Pa•m^2)	K_{r1} (N•m)	K_{r2} (N•m)	K_{s1} (N/m)	K_{s2} (N/m)
Cable 1	Accurate value	2.9036*E*6	7.9197*E*4	1.2552*E*8	1.5839*E*5	3.1679*E*5	3.9599*E*5	7.9197*E*5
	Initial value	2.3229*E*6	6.3358*E*4	1.0042*E*8	7.9197*E*4	1.5839*E*5	1.9799*E*5	3.9599*E*5
	Initial error (%)	20	20	20	50	50	50	50
Cable 2	Accurate value	7.2590*E*05	7.9222*E*04	1.3080*E*08	1.5844*E*05	3.1689*E*5	3.9611*E*5	7.9222*E*5
	Initial value	5.8072*E*05	6.3378*E*04	1.0464*E*08	7.9222*E*4	1.5844*E*5	1.9806*E*5	3.9611*E*5
	Initial error (%)	20	20	20	50	50	50	50
Cable 3	Accurate value	2.6133*E*7	1.0244*E*8	1.6371*E*11	2.0488*E*8	4.0976*E*8	5.1220*E*8	1.0244*E*9
	Initial value	2.0906*E*7	8.1952*E*7	1.3097*E*11	1.0244*E*8	2.0488*E*8	2.5610*E*8	5.1220*E*8
	Initial error (%)	20	20	20	50	50	50	50
Cable 4	Accurate value	7.2590*E*5	2.8464*E*6	1.3080*E*8	5.6928*E*6	1.1386*E*7	1.4232*E*7	2.8464*E*7
	Initial value	5.8072*E*5	2.2771*E*6	1.0464*E*8	2.8464*E*6	5.6928*E*6	7.1160*E*6	1.4232*E*7
	Initial error (%)	20	20	20	50	50	50	50

Table 3: Accurate modal frequencies of the four cables (Hz).

No	1st-order	2nd-order	3rd-order	4th-order	5th-order	6th-order	7th-order
Cable 1	0.420	0.821	1.232	1.644	2.057	2.470	2.885
Cable 2	0.410	0.431	0.648	0.850	1.063	1.275	1.488
Cable 3	1.374	2.671	4.044	5.459	6.932	8.472	10.092
Cable 4	0.414	0.445	0.678	0.909	1.154	1.411	1.682

support stiffnesses K_s were infinity, the static profiles of the cables with different K_r (i.e., EI/a, 2 EI/a, 4 EI/a, and ∞) were calculated and compared, as shown in Figure 6(a). It could be seen that the static deformation of the cable declined with the increase of K_r. However, generally speaking, K_r exhibited a slight effect on the cable's static profile.

Next, as depicted in Figure 6(b), the effect of the lateral support stiffnesses at the cable ends on the cable's static profile was analyzed, taking Cable 2 as an example. Analogously, the boundary lateral support stiffnesses K_s were assumed to be the same at the two ends, and the boundary rotational stiffnesses K_r at the two ends were both set as EI/a. Five conditions were analyzed, namely, K_s = EI/a^3, 2 EI/a^3, 4 EI/a^3, 8 EI/a^3, and ∞, respectively. One can find that with the decrease of K_s, the cable's static profile presented an approximate overall translation, in addition to the increase of the static deformation of the cable. Moreover, when K_s became larger, the sensitivity of the cable's static profile to K_s decreased.

4.2.2. Influence on Cable's Vibration Frequencies. As shown in Figure 7, the first two frequencies of the vibration of each cable under different boundary conditions were calculated and compared, to learn the influence of the boundary on the cable's vibration characteristics. Noteworthy is that the boundary constraints at the two cable ends were assumed to be the same during the analysis.

First, keeping the lateral support stiffness K_s being infinity, the first two frequencies of the cables with different boundary rotational stiffnesses K_r (i.e., 0, EI/a, 2 EI/a, and ∞) were compared. One can find in Figure 7 that K_r had a significant influence on Cables 3 and 4 with large flexural stiffnesses, which indicated that the sensitivity of the cable vibration frequency to K_r is affected by the flexural stiffness of the cable. However, larger sag would weaken the influence of K_r. For example, the frequencies of Cable 4 with large sag showed weaker sensitivity to K_r compared to Cable 3 with small sag. These results proved that K_r mainly affects the dynamic characteristics of the cables with large flexural stiffness but small sag.

Then, keeping the rotational stiffness K_r at boundary being EI/a, the first two frequencies of the cables with different lateral support stiffnesses K_s (i.e., EI/a^3, 2 EI/a^3, 10 EI/a^3, and ∞) were also compared. It could be found in Figure 7 that the K_s presented a complex influence on the cables' vibration frequencies. With the increase of K_s: the frequencies of Cables 1 and 2 increased significantly; the frequencies of Cable 3 decreased slightly; and the frequencies of Cable 4 did not change much. The reason could be found in the expressions of the elements Q, T, R, and P within the stiffness matrix $\mathbf{K_1}$ shown in equations (29)–(32). One can find that there is a common term $\mathrm{EI} \cdot H - K_r^2$ in the numerators and denominators of these equations and the term K_s appears only in the denominators. Therefore, the size relationship between K_r^2 and $EI \cdot H$ will determine the influence of K_s on the elements Q, T, R, and P within the stiffness matrix $\mathbf{K_1}$ and further the cables' vibration frequencies.

4.3. Validation of Eigenvalue Derivative Calculation Results. As stated before, the calculation of the vibration eigenvalue derivatives $\partial\lambda_n/\partial x_k$ is the key aspect of the calculation of matrix $\boldsymbol{\alpha}$. To verify the derived equations for computing the eigenvalue derivatives, the eigenvalue derivatives were first transformed into frequency derivatives using the following equation derived from $\lambda = \omega^2 = (2\pi f)^2$,

$$\frac{\partial f}{\partial x_k} = \frac{1}{8\pi^2 f} \frac{\partial \lambda}{\partial x_k}. \tag{43}$$

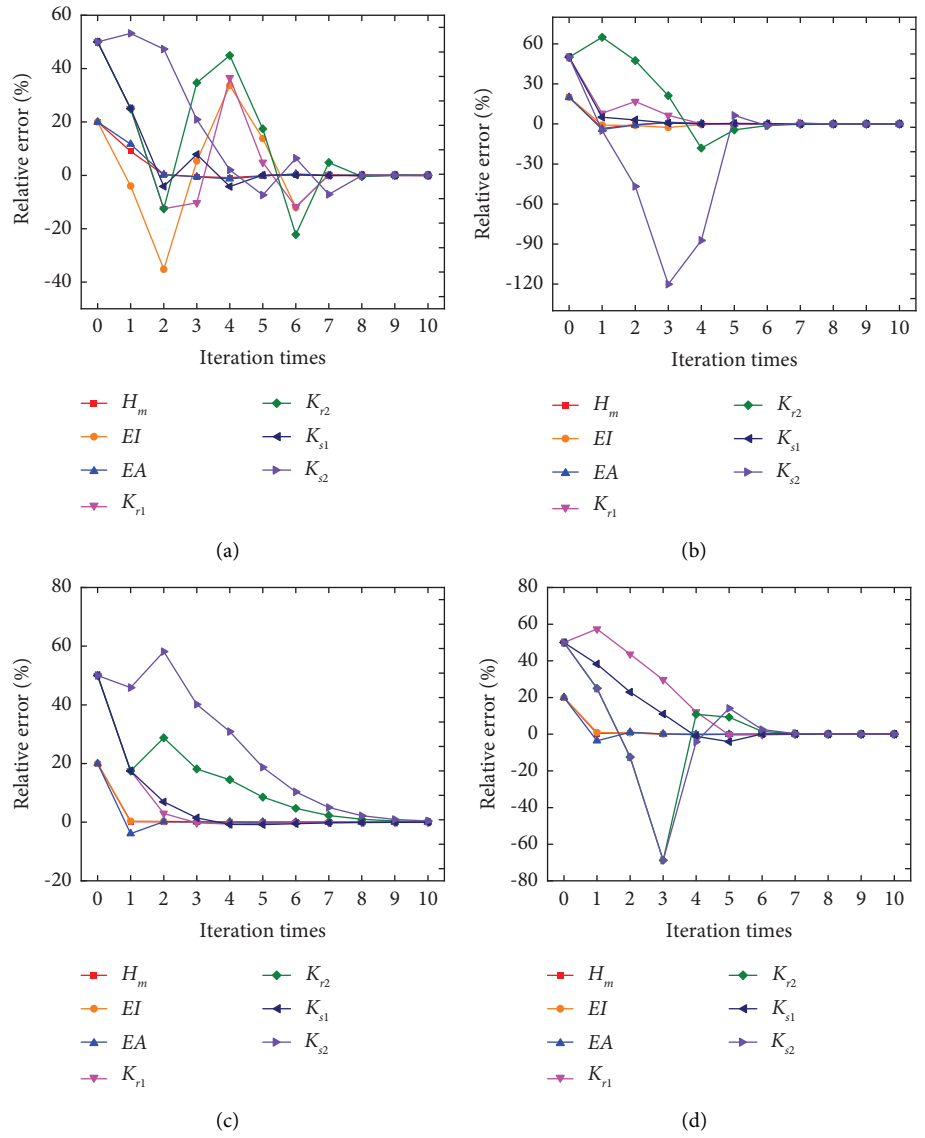

Figure 9: Convergence of the relative errors of cable system parameters with iteration times: (a) Cable 1; (b) Cable 2; (c) Cable 3; and (d) Cable 4.

Then, the calculated frequency derivatives with respect to each cable parameter were presented visually in the form of tangents at several selected points on the frequency-parameter curve (i.e., f-x_k curve). Taking Cable 2 as an example, the derivatives of the first-order frequency with respect to its multiple system parameters were calculated and illustrated in Figure 8 (due to the limited space, the derivatives of the frequencies of the other orders were not shown here). It could be seen that the calculated tangents (blue short solid lines) had good agreement with the actual curve slopes on each frequency-parameter curve, proving the accuracy of the analytical method for calculating $\partial\lambda_n/\partial x_k$ derived in this article.

Noteworthy is that, when obtaining the curves that frequency varies with H_m, EI, and EA, respectively, in Figure 8, the boundary conditions of the cable were assumed to be fixed at the two ends; when obtaining the curve that frequency varies with K_r, it was assumed that the boundary constraints at the two cable ends were the same and K_s were infinity; and when obtaining the curve that frequency varies with K_s, it was assumed that the boundary constraints at the two cable ends were the same and $K_r = \mathrm{EI}/a$.

4.4. Multiparameter Identification of the Cable

4.4.1. Model Setup. The four numerical cables in Table 1 were adopted to illustrate the effectiveness of the frequency-based sensitivity-updating algorithm for identifying multiple system parameters using the multiorder frequencies. To consider the effects of elastic embedding and elastic support at the cable boundary, for all four cables, assume that the accurate values of the rotational constraint stiffnesses (K_{r1} and K_{r2}) at the two ends of the cables were 2 EI/a and 4 EI/a, respectively, and that the accurate values of the lateral support stiffness (K_{s1} and K_{s2}) at the two ends of the cables were 5 EI/a^3 and 10 EI/a^3,

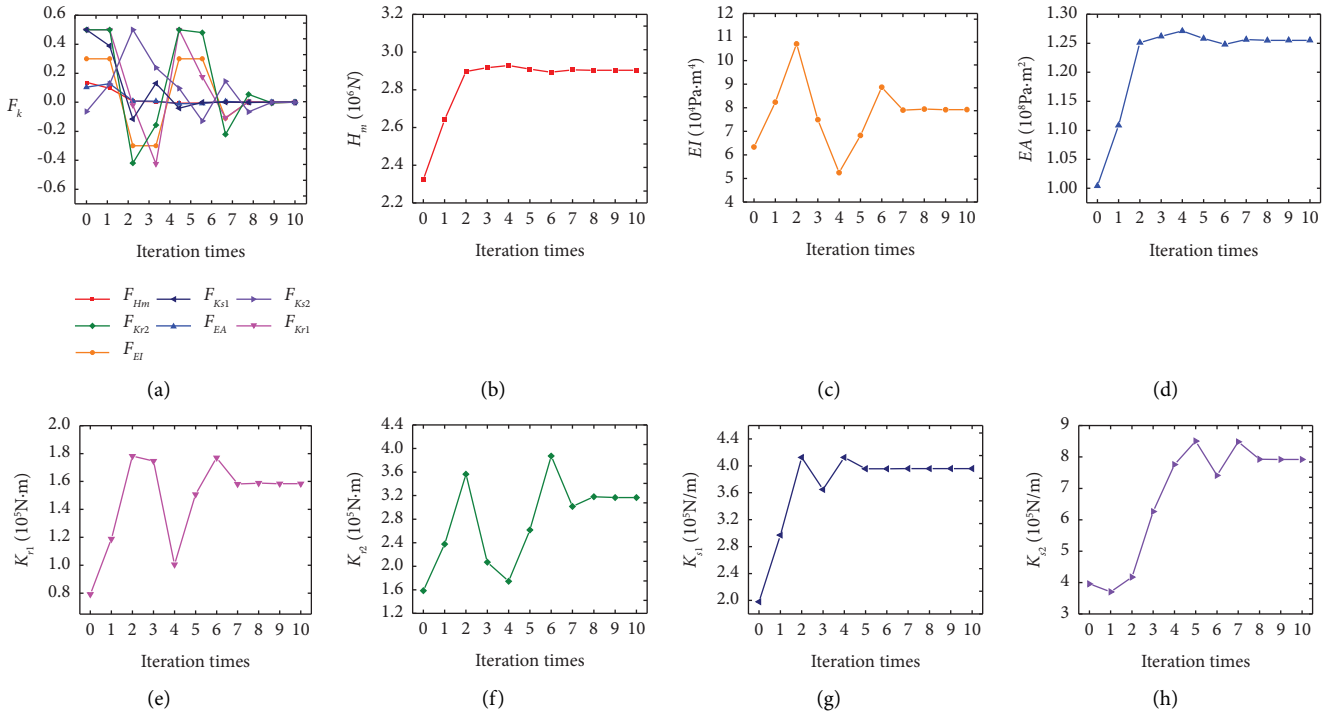

FIGURE 10: Convergence of (a) correction coefficients F_k, (b) H_m, (c) EI, (d) EA, (e) K_{r1}, (f) K_{r2}, (g) K_{s1}, and (h) K_{s2} of cable 1 during the identification process.

respectively. Moreover, in the first iteration, it was assumed that the errors of the initial iteration values of H_m^{eva}, EI^{eva}, and EA^{eva} of each cable were all 20%, and the errors of the initial iteration values of K_{r1}^{eva}, K_{r2}^{eva}, K_{s1}^{eva}, and K_{s2}^{eva} of each cable were all 50%, as shown in Table 2. The accurate frequencies of the cables, f_{mn}, which should be measured in the field in practical engineering, were calculated from the accurate system parameters in Table 2 in this paper, as listed in Table 3.

4.4.2. Results. Using the method described in Section 3.5, the identification of the multiple system parameters of the four numerical cables was complemented based on their true model frequencies listed in Table 3. In order to enhance the robustness of the iteration, the variation ranges of F_{H_m}, F_{EI}, and F_{EA} were constrained to within [−0.3, +0.3], and the variation ranges of $F_{K_{r1}}$, $F_{K_{r1}}$, $F_{K_{s1}}$, and $F_{K_{s2}}$ were constrained to within [−0.5, +0.5].

Figure 9 shows the convergence process of the relative errors of cable system parameters with the iteration times. It can be observed that the cable system parameters obtained after the first iteration still had relatively large errors. After a total of 10 iterations, the relative errors of cable system parameters converged to zero for all four cables. At this time, the system parameters tended to be stable and to converge to the accurate values. The abovementioned results indicated that the frequency-based sensitivity-updating algorithm could be adopted to identify the multiple system parameters quickly and effectively for different kinds of cables.

To give more details, taking Cable 1 as an example, the convergence of the correction coefficients and system parameters of Cable 1 is shown in Figure 10. It could be seen

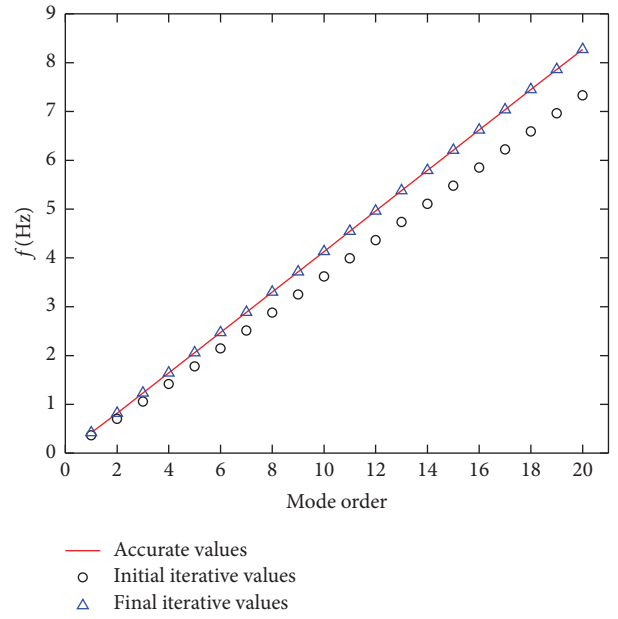

FIGURE 11: Comparison of iteration results with accurate values of modal frequencies of cable 1.

that, among the system parameters of the cable, H_m and EA converged faster. After 3 iterations, their identification errors were less than 0.5%. In contrast, the other system parameters converged relatively slowly. After 8 iterations, the identification errors of all system parameters were less than 0.5%. Figure 11 depicts the comparison between the frequencies calculated from the initial iterative values, final

iterative values, and accurate values of the cable parameters, respectively. It can be observed that the errors of the frequencies calculated from the initial iterative values of the system parameters were very large. After repeated iterations, the frequencies calculated from the final iterative values showed good agreement with the accurate frequencies. This also illustrated the effectiveness of the frequency-based sensitivity-updating algorithm.

5. Concluding Remarks

A nonlinear mathematical model of the vibration of the cable was established in this study with a systematical and comprehensive consideration of the influence of the inclination, bending stiffness, and sag-extensibility of the cable, particularly of the rotational constraint stiffness and the lateral support stiffness at the cable ends. The finite difference method was used to discretize the cable model, and the expressions of the linear stiffness matrix and the nonlinear stiffness matrix of the cable were strictly derived. Finally, a frequency-based sensitivity-updating algorithm was applied to identify multiple system parameters of the cable according to multiple frequencies. The results obtained made it possible to draw the following conclusions:

(1) The frequency-based sensitivity-updating algorithm can simultaneously and accurately identify the system parameters for different kinds of cables utilizing multiple frequencies;

(2) Calculation of the derivatives of the eigenvalues of the cable vibration is a key to obtaining the system sensitivity matrix. The developed calculation formulae were proved to be able to calculate accurately the derivatives of the vibration eigenvalues of an inclined cable;

(3) To enhance the robustness of the sensitivity-updating algorithm during the iteration, the variation range of the cable parameter could be constrained to a proper interval;

(4) The cable's boundary conditions have a complex influence on the static and dynamic characteristics of the cable: the rotational stiffness K_r exhibits a slight effect on the cable's static profile but the variation of lateral support stiffnesses K_s will cause an approximate overall static profile translation; K_r mainly affects the frequencies of the cables with large flexural stiffness but small sag; and the size relationship between K_r^2 and $\mathrm{EI} \cdot H$ will determine the influence of K_s on frequencies. It is necessary to take into account the effects of boundary conditions of the cable for the estimation of the cable tension.

Appendix

Eigenvalue Derivative Calculation

The eigenvalue derivative of the matrix plays an important role in updating the model [16]. In the following, the analytical method to compute the eigenvalue derivatives is introduced.

To obtain the derivatives of the vibration eigenvalues, equation (20) adopts the following form:

$$[\mathbf{K}(\mathbf{X}) - \lambda(\mathbf{X})\mathbf{M}(\mathbf{X})]\mathbf{w}(\mathbf{X}) = 0, \tag{A.1}$$

in which, $\lambda(\mathbf{X}) = \omega^2(\mathbf{X})$. Assume that λ_1 and $\mathbf{w}_1$ are an eigenvalue and its corresponding eigenvector of the above-mentioned eigenvalue equation, respectively, when $\mathbf{X} = \mathbf{X}^*$. Based on equation (A.1), Ma [17] derived the following equation for computing eigenvalue derivatives:

$$\frac{\partial \lambda_1(\mathbf{X}^*)}{\partial x_k} = \left[\mathbf{w}_1^{\mathrm{T}}\mathbf{M}\mathbf{w}_1\right]^{-1}\mathbf{w}_1^{\mathrm{T}}\left[\lambda_1\frac{\partial \mathbf{M}}{\partial x_k} - \frac{\partial \mathbf{K}(\mathbf{X}^*)}{\partial x_k}\right]\mathbf{w}_1. \tag{A.2}$$

Equation (A.2) shows that it is essential to compute the derivative of the stiffness matrix, $\partial\mathbf{K}/\partial x_k$, and the derivative of the mass matrix, $\partial\mathbf{M}/\partial x_k$, of the cable to solve the eigenvalue derivatives of cable vibration. It is easy to find that $\partial\mathbf{M}/\partial x_k = 0$. Differentiating each element in the linear stiffness matrix $\mathbf{K}_1$ directly, the derivative of $\mathbf{K}_1$ with respect to x_k can be determined. The derivatives of each element in $\mathbf{K}_1$ with respect to x_k are as follows (due to the limited space, the derivatives of the elements T and P are not given here, which have similar forms with those of elements Q and R, respectively, and can be obtained by proper mathematical derivation):

$$\frac{\partial S}{\partial(H)} = \frac{2}{a^2}, \frac{\partial S}{\partial(EI)} = \frac{6}{a^4}, \frac{\partial D}{\partial(H)} = -\frac{1}{a^2}, \frac{\partial D}{\partial(EI)} = -\frac{4}{a^4},$$

$$\frac{\partial U}{\partial(H)} = -\frac{1}{a^2}, \frac{\partial U}{\partial(EI)} = -\frac{4}{a^4}, \frac{\partial V}{\partial(EI)} = \frac{1}{a^4}, \frac{\partial W}{\partial(EI)} = \frac{1}{a^4}, \tag{A.3}$$

$$\begin{aligned}\frac{\partial Q}{\partial(EI)} &= \frac{6}{a^4}+\frac{K_{r1}a-2EI_0}{a^4\left(K_{r1}a+2EI_0\right)}-\frac{4K_{r1}a}{\left(K_{r1}a+2EI_0\right)^2}V_1\\ &+\frac{2K_{s1}K_{r1}a\left(H_0a+K_{r1}\right)}{\left[K_{s1}a\left(K_{r1}a+2EI_0\right)+2EI_0H_0-2K_{r1}^2\right]^2}\left(D_1+\frac{4EI_0}{K_{r1}a+2EI_0}V_1\right)\\ &+\frac{2EI_0H_0-2K_{r1}^2}{K_{s1}a\left(K_{r1}a+2EI_0\right)+2EI_0H_0-2K_{r1}^2}\left[\frac{-4}{a^4}+\frac{4EI_0}{a^4\left(K_{r1}a+2EI_0\right)}+\frac{4K_{r1}a}{\left(K_{r1}a+2EI_0\right)^2}V_1\right],\end{aligned} \tag{A.4}$$

$$\begin{aligned}\frac{\partial Q}{\partial(H)} &= \frac{2}{a^2}+\left(-\frac{1}{a^2}\right)\frac{2EI_0H_0-2K_{r1}^2}{K_{s1}a\left(K_{r1}a+2EI_0\right)+2EI_0H_0-2K_{r1}^2}\\ &+\frac{2EI_0K_{s1}a\left(K_{r1}a+2EI_0\right)}{\left[K_{s1}a\left(K_{r1}a+2EI_0\right)+2EI_0H_0-2K_{r1}^2\right]^2}\left(D_1+\frac{4EI_0}{K_{r1}a+2EI_0}V_1\right),\end{aligned} \tag{A.5}$$

$$\begin{aligned}\frac{\partial Q}{\partial\left(K_{r1}\right)} &= \frac{K_{s1}a\left(K_{r1}a+2EI_0\right)}{K_{s1}a\left(K_{r1}a+2EI_0\right)+2EI_0H_0-2K_{r1}^2}\cdot\frac{4EI_0a}{\left(K_{r1}a+2EI_0\right)^2}V_1\\ &-\frac{4K_{s1}K_{r1}a\left(K_{r1}a+2EI_0\right)+K_{s1}a^2\left(2EI_0H_0-2K_{r1}^2\right)}{\left[K_{s1}a\left(K_{r1}a+2EI_0\right)+2EI_0H_0-2K_{r1}^2\right]^2}\left(D_1+\frac{4EI_0}{K_{r1}a+2EI_0}V_1\right),\end{aligned} \tag{A.6}$$

$$\frac{\partial Q}{\partial\left(K_{s1}\right)} = -\frac{a\left(K_{r1}a+2EI_0\right)\left(2EI_0H_0-2K_{r1}^2\right)}{\left[K_{s1}a\left(K_{r1}a+2EI_0\right)+2EI_0H_0-2K_{r1}^2\right]^2}\left(D_1+\frac{4EI_0}{K_{r1}a+2EI_0}V_1\right), \tag{A.7}$$

$$\frac{\partial R}{\partial(EI)} = -\frac{4}{a^4}+\frac{1}{a^4}\cdot\frac{2EI_0H_0-2K_{r1}^2}{K_{s1}a\left(K_{r1}a+2EI_0\right)+2EI_0H_0-2K_{r1}^2}+\frac{2K_{s1}K_{r1}a\left(H_0a+K_{r1}\right)}{\left[K_{s1}a\left(K_{r1}a+2EI_0\right)+2EI_0H_0-2K_{r1}^2\right]^2}V_2, \tag{A.8}$$

$$\frac{\partial R}{\partial(H)} = -\frac{1}{a^2}+\frac{2EI_0K_{s1}a\left(K_{r1}a+2EI_0\right)}{\left[K_{s1}a\left(K_{r1}a+2EI_0\right)+2EI_0H_0-2K_{r1}^2\right]^2}V_2, \tag{A.9}$$

$$\frac{\partial R}{\partial\left(K_{r1}\right)} = -\frac{4K_{s1}K_{r1}a\left(K_{r1}a+2EI_0\right)+K_{s1}a^2\left(2EI_0H_0-2K_{r1}^2\right)}{\left[K_{s1}a\left(K_{r1}a+2EI_0\right)+2EI_0H_0-2K_{r1}^2\right]^2}V_2, \tag{A.10}$$

$$\frac{\partial R}{\partial\left(K_{s1}\right)} = -\frac{a\left(K_{r1}a+2EI_0\right)\left(2EI_0H_0-2K_{r1}^2\right)}{\left[K_{s1}a\left(K_{r1}a+2EI_0\right)+2EI_0H_0-2K_{r1}^2\right]^2}V_2. \tag{A.11}$$

It should be noted from the expression of $\mathbf{K}_1$ that $\partial\mathbf{K}_1/\partial(EA)=0$.

Similarly, the derivative of the nonlinear stiffness matrix $\mathbf{K}_2$ with respect to the system parameters can be obtained by

$$\frac{\partial\mathbf{K}_2(i,j)}{\partial x_k} = \frac{\partial\left(\mathbf{r}_i\mathbf{s}_j^{\mathrm{T}}\right)}{\partial x_k} = \frac{\partial\mathbf{r}_i}{\partial x_k}\mathbf{s}_j^{\mathrm{T}}+\mathbf{r}_i\frac{\partial\mathbf{s}_j^{\mathrm{T}}}{\partial x_k}\ (i,j=1,2,\ldots,n), \tag{A.12}$$

where

$$\frac{\partial s_j}{\partial x_k} = \frac{1}{a^2}\left[\frac{\partial y_{j+1}}{\partial x_k} - 2\frac{\partial y_j}{\partial x_k} + \frac{\partial y_{j-1}}{\partial x_k}\right], \tag{A.13}$$

$$\frac{\partial r_i}{\partial x_k} = \frac{\partial s_i}{\partial x_k} EA_i \left(\sum_{i=1}^{n} t_i^3\right)^{-1} - s_i EA_i \left(\sum_{i=1}^{n} t_i^3\right)^{-2} \sum_{i=1}^{n}\left(3t_i^2 \frac{\partial t_i}{\partial x_k}\right), \tag{A.14}$$

$$\frac{\partial t_i}{\partial x_k} = \frac{1}{2a}\left[\left(\frac{y_{i+1} - y_{i-1}}{2a}\right)^2 + 1\right]^{-1/2}\left(\frac{\partial y_{i+1}}{\partial x_k} - \frac{\partial y_{i-1}}{\partial x_k}\right)\left(\frac{y_{i+1} - y_{i-1}}{2a}\right). \tag{A.15}$$

It can be seen that the derivative of each element in the stiffness matrix $\mathbf{K}_2$ is related to the static displacement derivative of the cable concerning the system parameters. To obtain the static displacement derivative of the cable, the following formula is considered:

$$\frac{\partial(\mathbf{K}_1\mathbf{Y})}{\partial x_k} = \mathbf{K}_1\frac{\partial \mathbf{Y}}{\partial x_k} + \frac{\partial \mathbf{K}_1}{\partial x_k}\mathbf{Y} = 0. \tag{A.16}$$

Therefore,

$$\frac{\partial \mathbf{Y}}{\partial x_k} = -\mathbf{K}_1^{-1}\frac{\partial \mathbf{K}_1}{\partial x_k}\mathbf{Y}, \tag{A.17}$$

where $\mathbf{Y}^T = \{y_1, y_2, \ldots, y_n\}$, y_i represents the static displacement of each node under static equilibrium.

Finally, the derivative of the overall stiffness matrix $\mathbf{K}$ with respect to the system parameters of the cable is as follows:

$$\frac{\partial \mathbf{K}}{\partial x_k} = \frac{\partial \mathbf{K}_1}{\partial x_k} + \frac{\partial \mathbf{K}_2}{\partial x_k}. \tag{A.18}$$

Data Availability

All data, models, and code generated or used during the study appear in the published article.

Conflicts of Interest

The authors declare that they have no conflicts of interest regarding the publication of this paper.

Acknowledgments

The work described in this paper was financially supported by the National Key R&D Program of China (Grant no. 2022YFB3706703), the National Natural Science Foundation of China (Grant no. 52078134), the Postgraduate Research & Practice Innovation Program of Jiangsu Province (Grant no. KYCX21_0118), and the Scientific Research Foundation of Graduate School of Southeast University (Grant no. YBPY2129), which are gratefully acknowledged.

References

[1] H. M. Irvine, *Cable Structures*, MIT Press, Cambridge, MA, USA, 1981.

[2] R. E. Clough and J. Penzien, *Dynamics of Structures*, McGraw-Hill, New York, NY, USA, 1993.

[3] H. Zui, T. Shinke, and Y. Namita, "Practical formulas for estimation of cable tension by vibration method," *Journal of Structural Engineering*, vol. 122, no. 6, pp. 651–656, 1996.

[4] W. X. Ren, G. Chen, and W. H. Hu, "Empirical formulas to estimate cable tension by cable fundamental frequency," *Structural Engineering & Mechanics*, vol. 20, no. 3, pp. 363–380, 2005.

[5] Z. Fang and J. Q. Wang, "Practical formula for cable tension estimation by vibration method," *Journal of Bridge Engineering*, vol. 17, no. 1, pp. 161–164, 2012.

[6] H. M. Irvine, T. K. Caughey, and G. B. Whitham, "The linear theory of free vibrations of a suspended cable," *Proceedings of the Royal Society of London, Series A: Mathematical and Physical Sciences*, vol. 341, no. 1626, pp. 299–315, 1974.

[7] T. Shimada and A. Nishimura, "Effect of flexural rigidity on cable tension estimated by vibration method," *Doboku Gakkai Ronbunshu*, vol. 1988, pp. 409–412, 1988.

[8] A. B. Mehrabi and H. Tabatabai, "Unified finite difference formulation for free vibration of cables," *Journal of Structural Engineering*, vol. 124, no. 11, pp. 1313–1322, 1998.

[9] B. F. Yan, J. Y. Yu, and M. Soliman, "Estimation of cable tension force independent of complex boundary conditions," *Journal of Engineering Mechanics*, vol. 141, no. 1, p. 8, Article ID 06014015, 2015.

[10] C. C. Chen, W. H. Wu, S. Y. Chen, and G. Lai, "A novel tension estimation approach for elastic cables by elimination of complex boundary condition effects employing mode shape functions," *Engineering Structures*, vol. 166, pp. 152–166, 2018.

[11] B. H. Kim and T. Park, "Estimation of cable tension force using the frequency-based system identification method," *Journal of Sound and Vibration*, vol. 304, no. 3-5, pp. 660–676, 2007.

[12] W. Y. Liao, Y. Q. Ni, and G. Zheng, "Tension force and structural parameter identification of bridge cables," *Advances in Structural Engineering*, vol. 15, no. 6, pp. 983–995, 2012.

[13] H. Li, F. J. Zhang, and Y. Z. Jin, "Real-time identification of time-varying tension in stay cables by monitoring cable transversal acceleration," *Structural Control and Health Monitoring*, vol. 21, no. 7, pp. 1100–1117, 2014.

[14] S. E. Zarbaf, M. Norouzi, R. J. Allemang, V. J. Hunt, and A. Helmicki, "Stay cable tension estimation of cable-Stayed bridges using genetic algorithm and particle swarm optimization," *Journal of Bridge Engineering*, vol. 22, no. 10, p. 9, Article ID 05017008, 2017.

[15] Y. Q. Ni, J. M. Ko, and G. Zheng, "Dynamic analysis of large-diameter sagged cables taking into account flexural rigidity," *Journal of Sound and Vibration*, vol. 257, no. 2, pp. 301–319, 2002.

[16] I. W. Lee and G. H. Jung, "An efficient algebraic method for the computation of natural frequency and mode shape sensitivities—Part I. Distinct natural frequencies," *Computers & Structures*, vol. 62, no. 3, pp. 429–435, 1997.

[17] L. Ma, "A highly precise frequency-based method for estimating the tension of an inclined cable with unknown boundary conditions," *Journal of Sound and Vibration*, vol. 409, pp. 65–80, 2017.